Advanced Glass Science
(4016101)

Instructor: Asst.Prof.Dr. Jakrapong Kaewkhao

Course Outline:

Week 11: Glass composition, structures and applications (3)
- Phosphate Glass
- Alkali-and Phosphate Glass
- *Case studies from international publications*

Book:
A.K., Varshneya. ***Fundamentals of inorganic glasses***
A., Paul A, ***Chemistry of glasses***
J.E. Shelby, ***Introduction to glass science and technology***

Phosphate Glasses

- Excellent host materials active RE ions due to advantageous local structure effect and high RE ion solubiity.

- Low refractive index

- Low vicosity

-melting temperature.

- High thermal stability

- Low optical dispersion

- High transparency

- Wide glass formation range

Alkali- and Akali Earth Phosphate Glasses

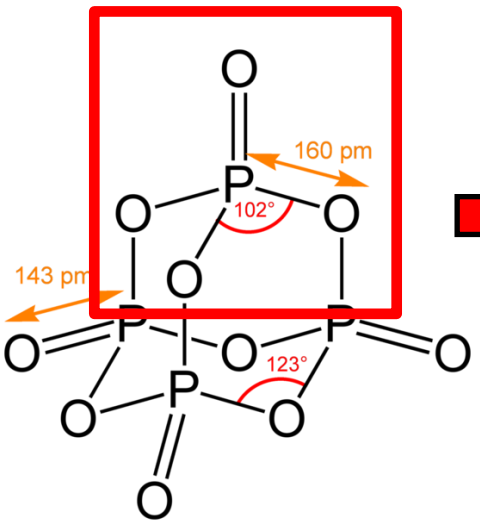

P_4O_{10} or (P_2O_5)

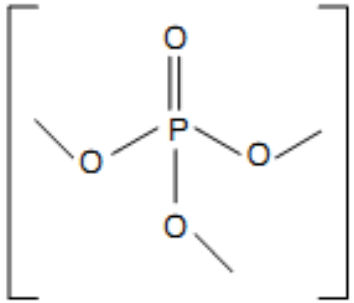

(Former)

+ CaO

(Modifier)

=

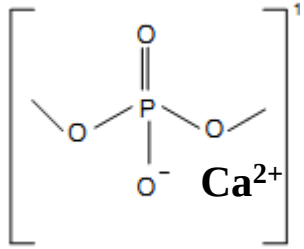

Metathophosphate

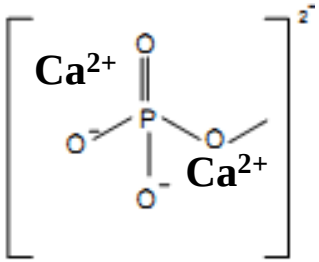

Pyrophosphate

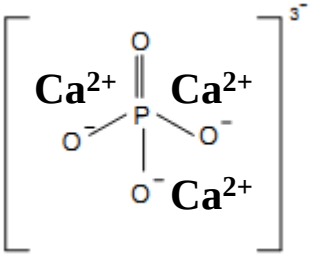

Orthophosphate

Binary Phosphate Glass

$$2Q^n + R_2O \rightarrow 2Q^{n-1}$$

In the ultraphosphate region $0 \leq x \leq 0.5$ the fraction of Q^2 and Q^3 tetrahedra are given by

$$f(Q^2) = \frac{x}{1-x},$$

$$f(Q^3) = \frac{1-2x}{1-x}$$

$$xR_2O \text{ (or } R'O) \ (1-x)P_2O_5$$

Metaphosphate glasses x ≐ 0:50 have networks based entirely on Q^2 tetrahedra that form chains and rings. The chains and rings are linked by more ionic bonds between various metal cations and the non-bridging oxygens. Because of the dic ulty in obtaining an exact stoichiometry, these compositions are usually more accurately described as long-chained polyphosphates.

Binary Phosphate Glass

Polyphosphate glasses (x > 0:50) have networks based on Q^2 chains terminated by Q^1 tetrahedra (one bridging and three non-bridging oxygens per tetrahedron). The average chain length becomes progressively shorter as the [O]/[P] ratio increases. At [O]/[P] = 3:5 (the pyrophosphate stoichiometry, x = 0:67), the network structure is dominated by phosphate dimers, two Q^1 tetrahedra linked by a common bridging oxygen. Glasses for which [O]/[P] > 3.5 contain isolated Q^0 (orthophosphate units) tetrahedra. Between the metaphosphate x = 0:50 and pyrophosphate x = 0:67 boundaries, the fraction of Q^1 and Q^2 tetrahedra are given by

$$f(Q^1) = \frac{2x - 1}{1 - x}$$

$$f(Q^2) = \frac{2 - 3x}{1 - x}$$

Binary Phosphate Glass

Between the pyrophosphate x..= 0:67†and orthophosphate (x ≏ 0:75) boundaries, the fraction of Q^0 and Q^1 tetrahedra are given by

$$f(Q^0) = \frac{3x - 2}{1 - x}$$

$$f(Q^1) = \frac{3 - 4x}{1 - x}$$

Binary Phosphate Glass

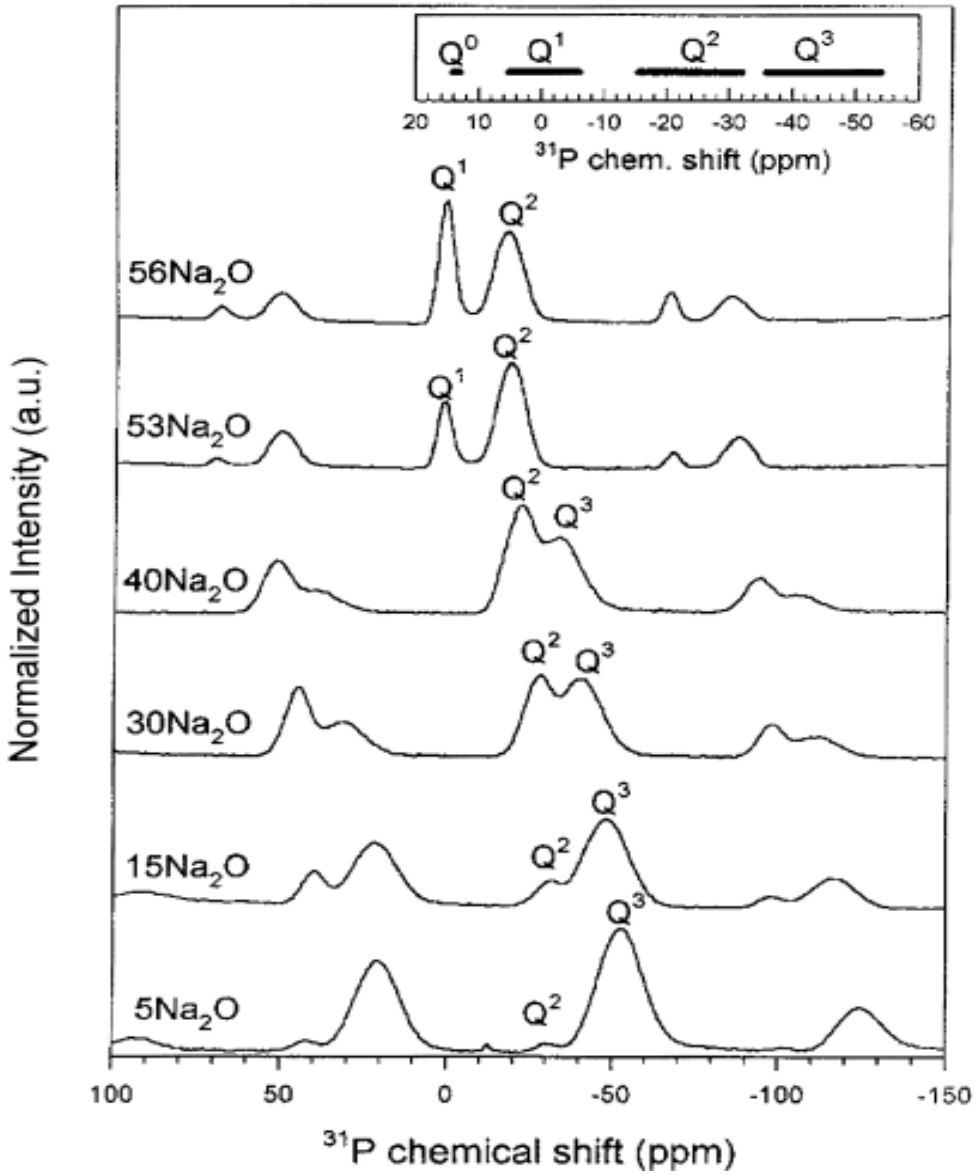

Fig. 1 ^{31}P NMR spectra from anhydrous Na phosphate glasses. Isotropic peaks that are due to different P-tetrahedra are labeled with the appropriate Q^i notation; the remaining peaks are spinning sidebands. The inset shows the range of chemical shifts reported for sodium phosphate glasses and crystals.

Contents lists available at ScienceDirect

Optical Materials

journal homepage: www.elsevier.com/locate/optmat

Investigation of spectroscopic properties (absorption and emission) of Ho^{3+} doped alkali, mixed alkali and calcium phosphate glasses

M. Seshadri [a], Y.C. Ratnakaram [a,*], D. Thirupathi Naidu [b], K. Venkata Rao [a]

Glass A : $(69.5P_2O_5 + 15Na_2O) + 15Li_2O + 0.5Ho_2O_3$

Glass B : $(69.5P_2O_5 + 15Na_2O) + 15Na_2O + 0.5Ho_2O_3$

Glass C : $(69.5P_2O_5 + 15Na_2O) + 15K_2O + 0.5Ho_2O_3$

Glass D : $(69.5P_2O_5 + 15Na_2O) + 7.5Li_2O + 7.5Na_2O + 0.5Ho_2O_3$

Glass E : $(69.5P_2O_5 + 15Na_2O) + 7.5Li_2O + 7.5K_2O + 0.5Ho_2O_3$

Glass F : $(69.5P_2O_5 + 15Na_2O) + 7.5Na_2O + 7.5K_2O + 0.5Ho_2O_3$

Glass G : $(69.5P_2O_5 + 15Na_2O) + 15CaO + 0.5Ho_2O_3$

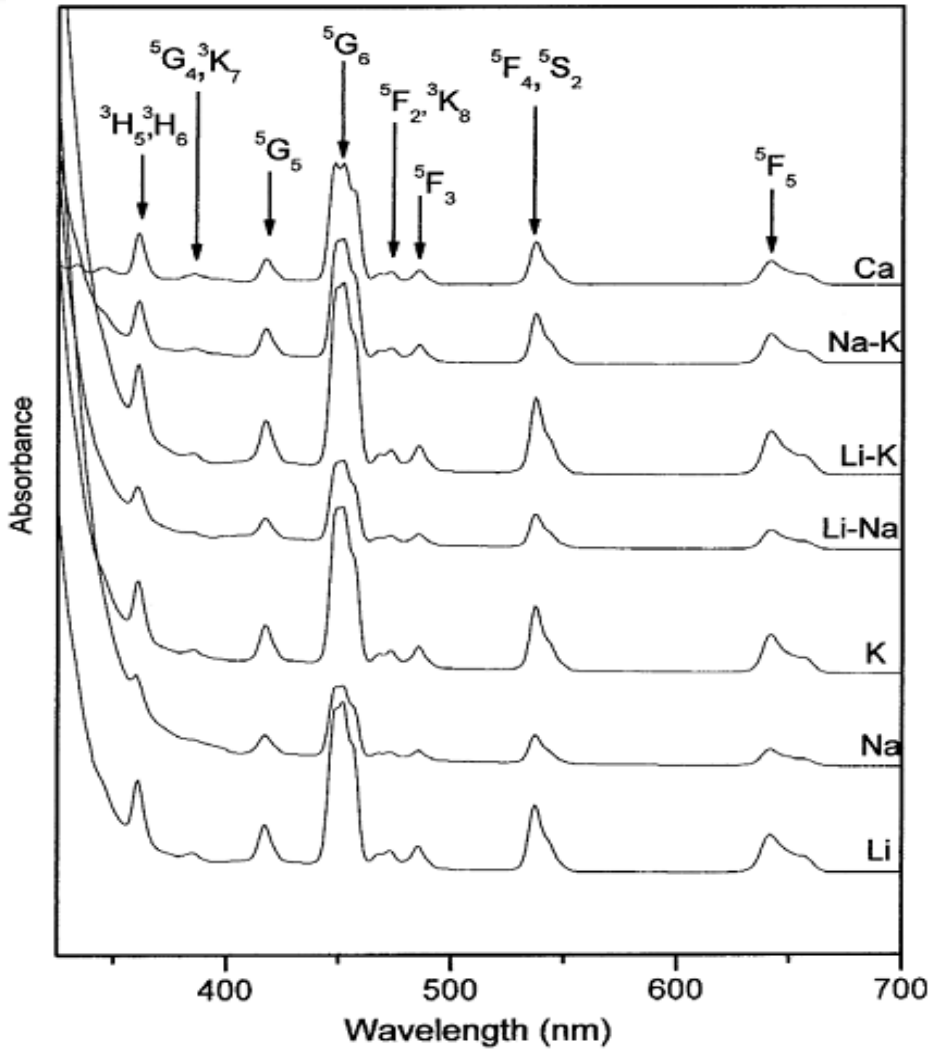

It is observed thatamong the four phosphate glass matrices (Li, Na, K and Ca), potassium glass and among the three mixed alkali phosphate glass matrices (Li–Na, Li–K and Na–K), lithium–potassium glass shows higher absorbance's indicating a strong electron–phonon interaction in the above two glass matrices

Fig. 2 Optical absorption spectra of Ho^{3+} doped alkali, mixed alkali and calcium phosphate glasses

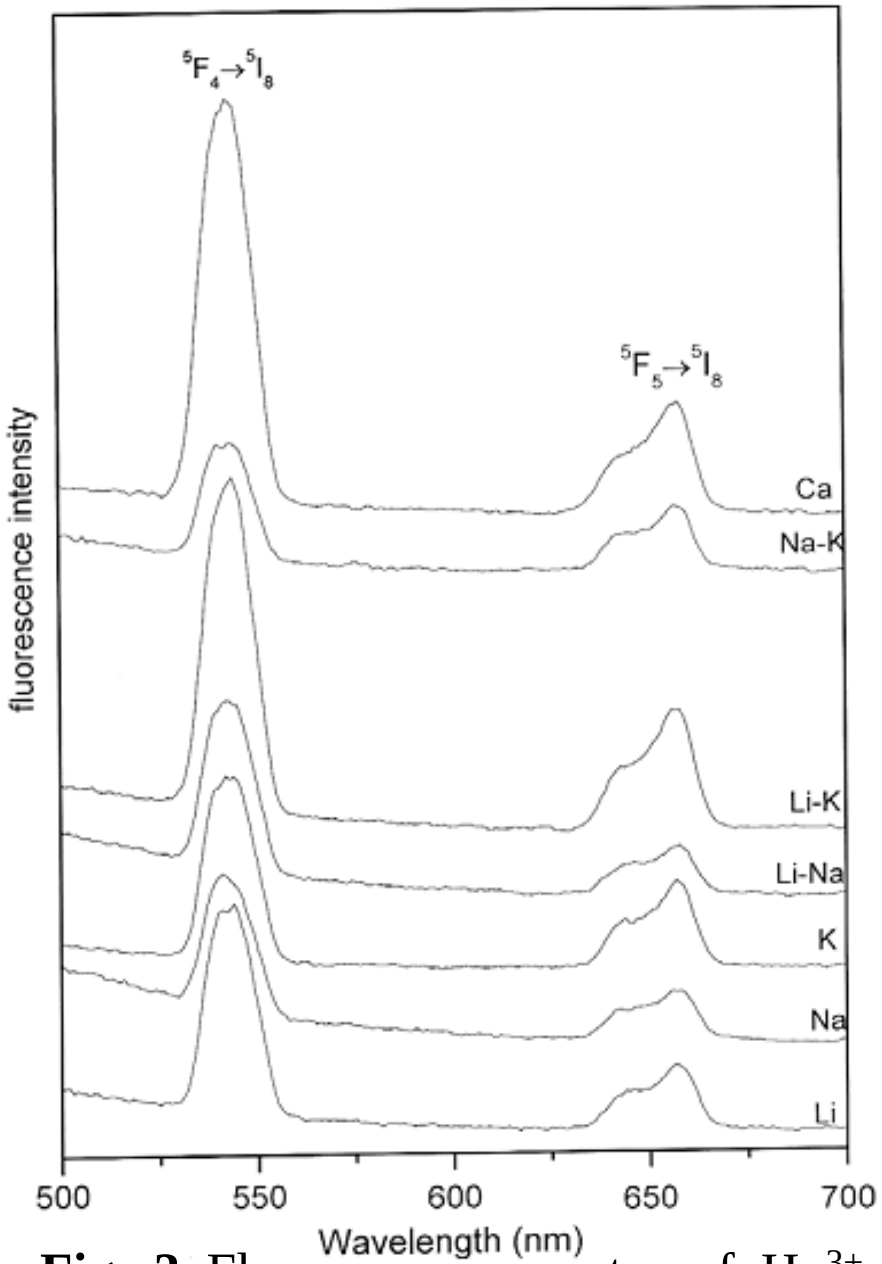

Fig. 3 Fluorescence spectra of Ho^{3+} doped alkali, mixed alkali and calcium inphosphate glasses.

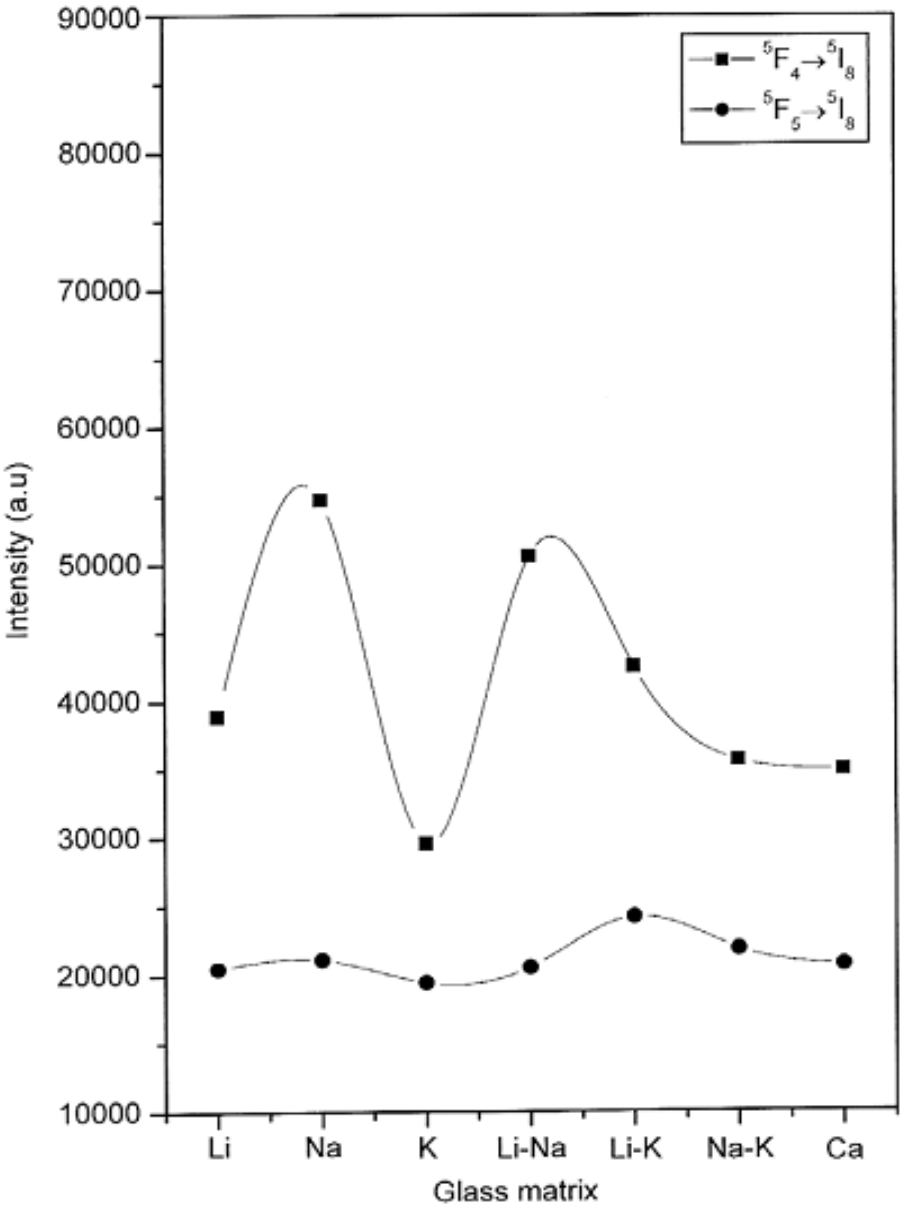

Fig. 4 Variation of emission intensity of the two peaks with the alkalis, mixed alkalis and calcium in phosphate glasses.

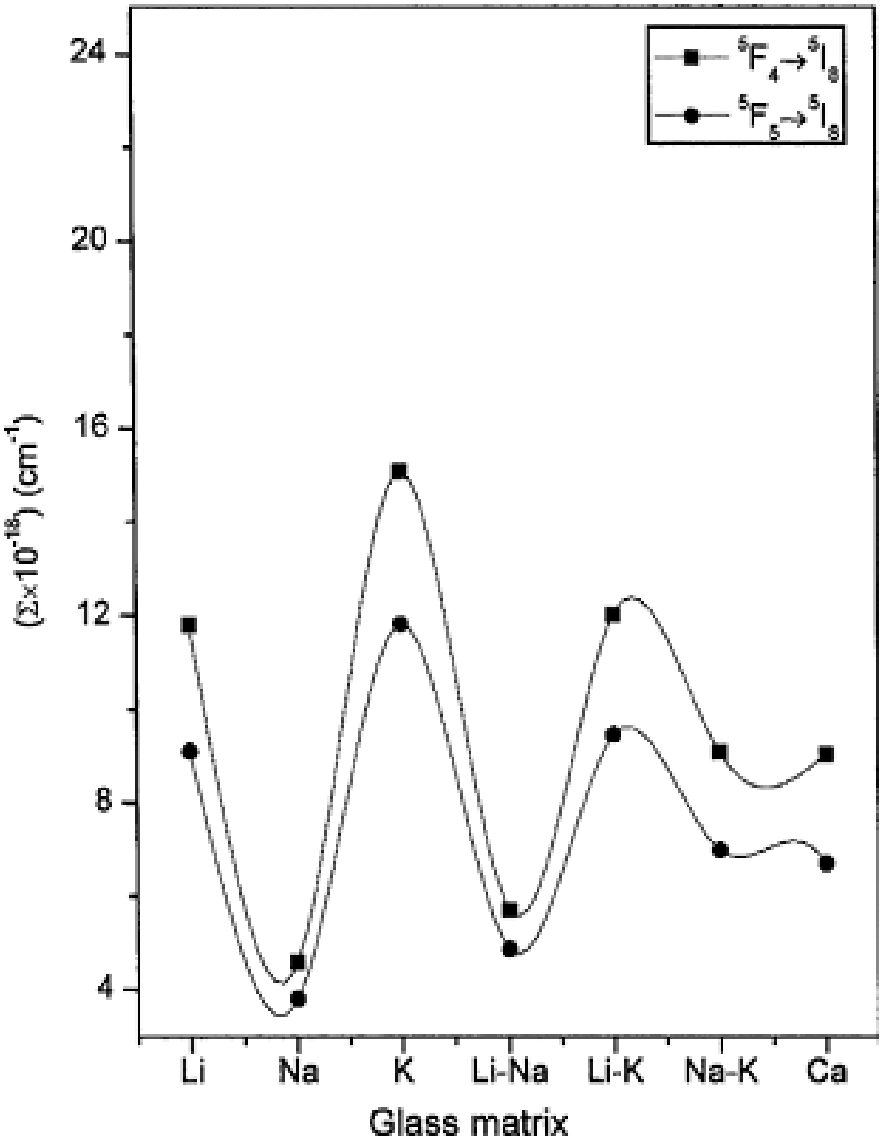

Fig. 5 Variation of absorption cross-sections of the transitions, $^5F_4 \rightarrow {}^5I_8$ and $^5F_5 \rightarrow {}^5I_8$ with the glass matrix.

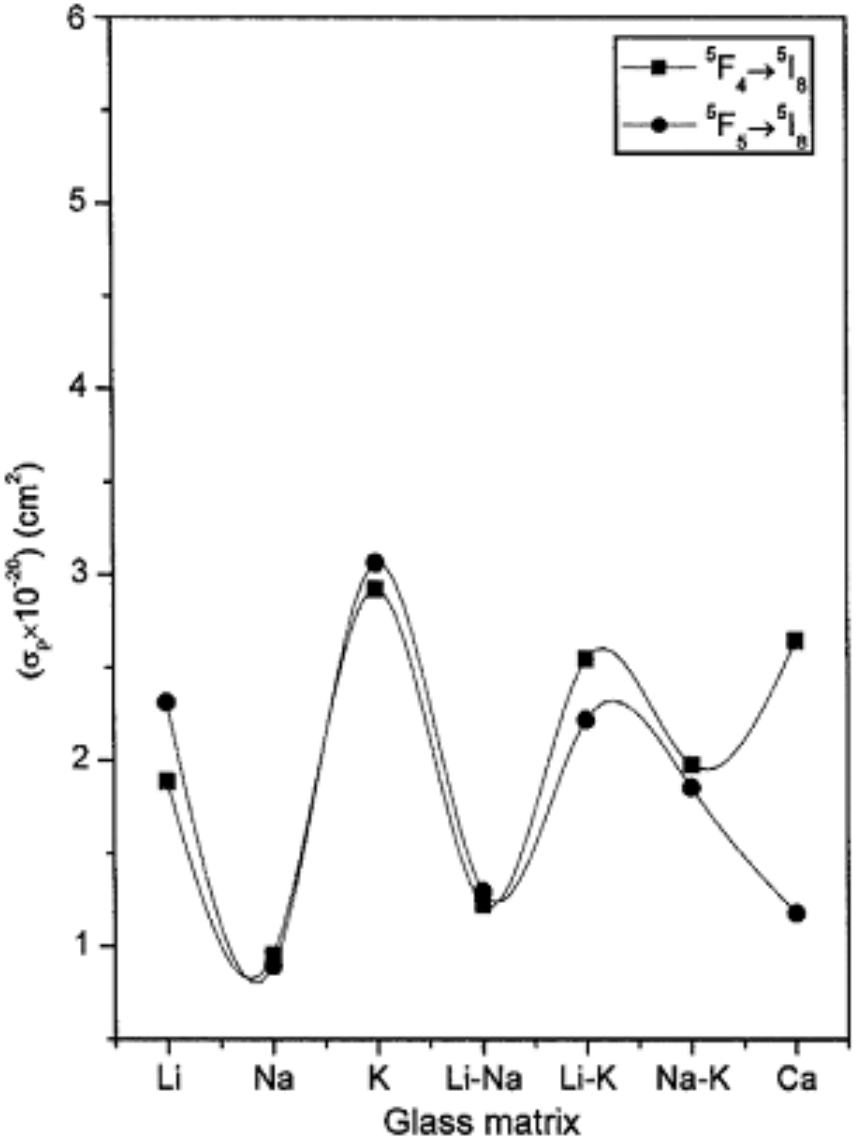

Fig. 6 Variation of absorption cross-sections of the transitions, $^5F_4 \rightarrow {}^5I_8$ and $^5F_5 \rightarrow {}^5I_8$ with the glass matrix.

Contents lists available at ScienceDirect

Journal of Luminescence

journal homepage: www.elsevier.com/locate/jlumin

Processes of the excitation energy migration and transfer in Ce^{3+}-doped alkali gadolinium phosphates studied with time-resolved photoluminescence spectroscopy technique

G. Stryganyuk [a,b,*], T. Shalapska [a,c], A. Voloshinovskii [a], A. Gektin [b], A. Krasnikov [c], S. Zazubovich [c]

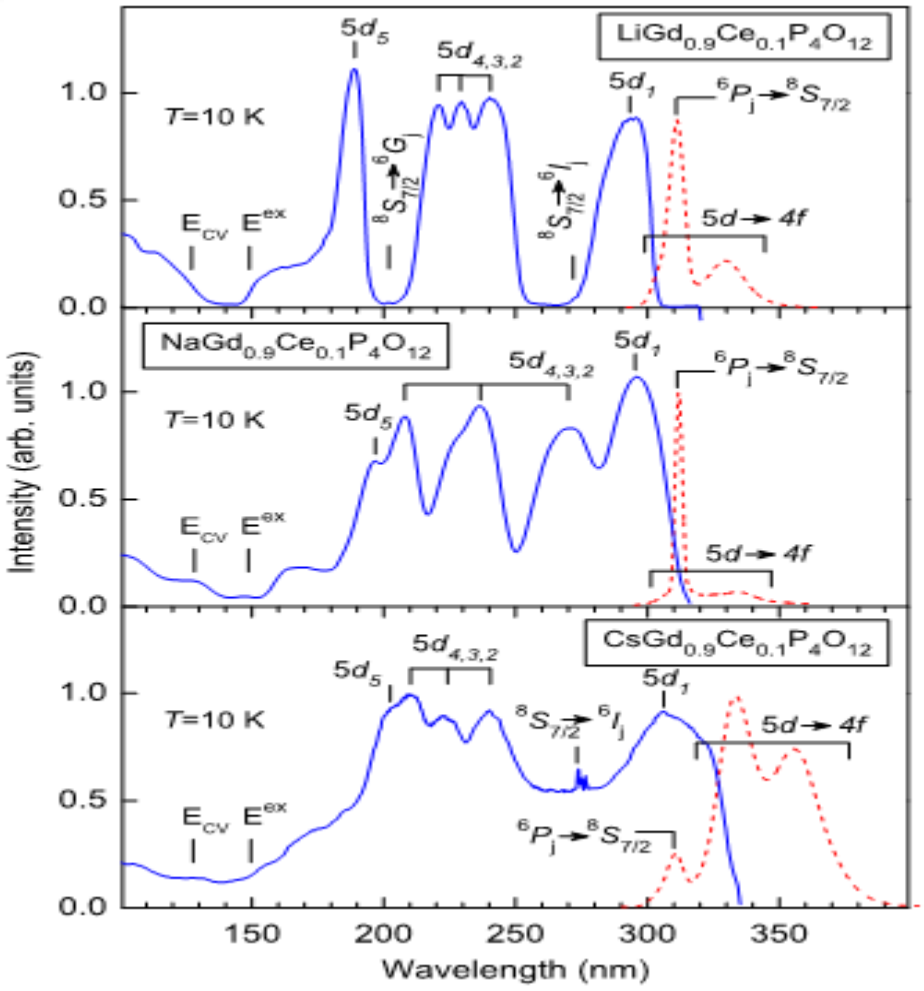

Fig. 7 Normalized luminescence excitation (solid lines, lem¼330 nm) and emission (dashed lines, excite at 220 nm) spectra of Ce^{3+}-doped $MGdP_4O_{12}$ (M = Li, Na, Cs) phosphates measured at T = 10 K

The characteristic spectral features of Gd^{3+} and Ce^{3+} luminescence from $LiGd_{0.9}Ce_{0.1}P_4O_{12}$, $NaGd_{0.9}Ce_{0.1}P_4O_{12}$, and $CsGd_{0.9}Ce_{0.1}P_4O_{12}$ phosphates upon excitation with the synchrotron radiation at T=10and 300 K are shown in Figs. 1 and 2, respectively (see also Table 1). The emission spectra presented in Figs. 1 and 2 (dashed lines) show that in all the phosphates studied, the short-wavelength band of Ce^{3+} 5d→4f emission doublet overlaps even at T=10 K strongly with the lowest-energy Gd^{3+} $^8S_{7/2} \leftrightarrow {}^6P_j$ transitions. The overlap of the Gd^{3+} $^6P_j \rightarrow {}^8S_{7/2}$ emission with the Ce^{3+} 4f→5d absorption (solid lines in Figs. 1 and 2) is enhanced with the temperature increase and it is found to increase for the $MGdP_4O_{12}$ phosphates series while the alkali ion is changed in Li, Na, Cs order.

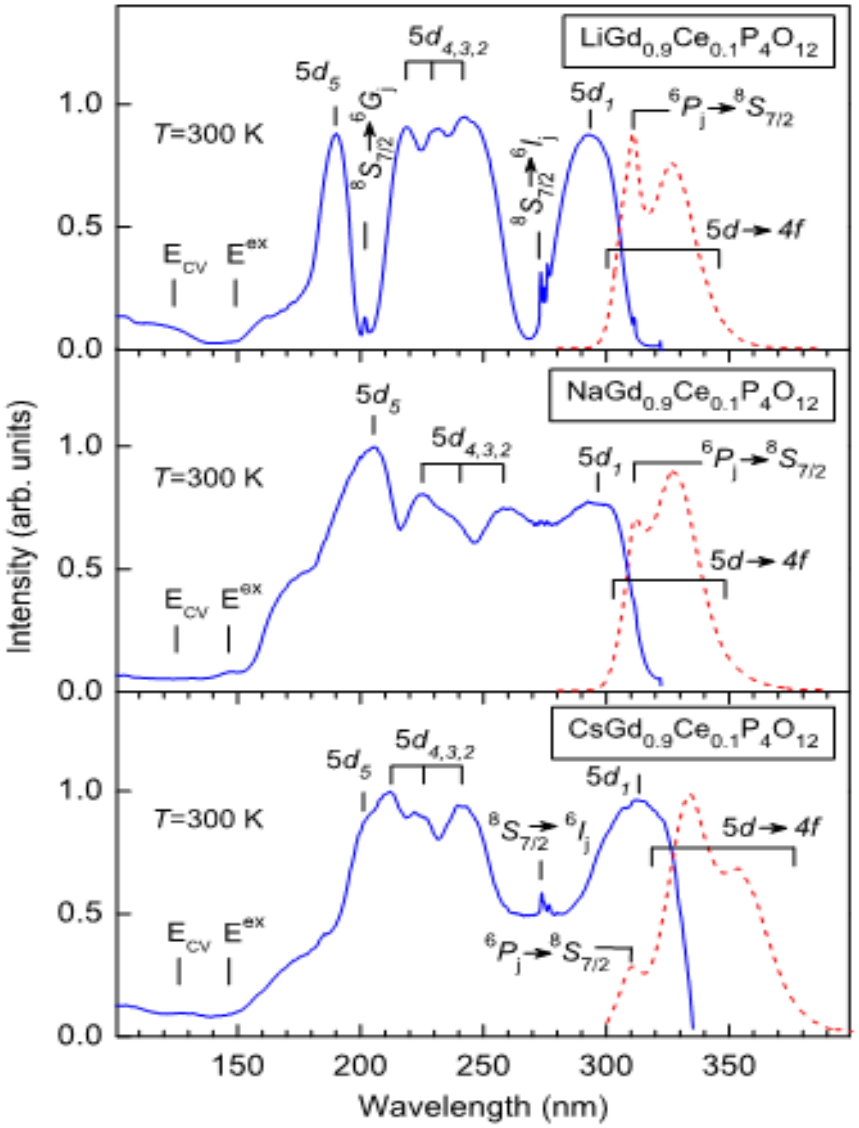

Fig. 8 Normalized luminescence excitation (solid lines, em = 330 nm) and emission (dashed lines, excite at 220 nm) spectra of Ce^{3+}-doped $MGdP_4O_{12}$ (M = Li, Na, Cs) phosphates measured at T = 10 K

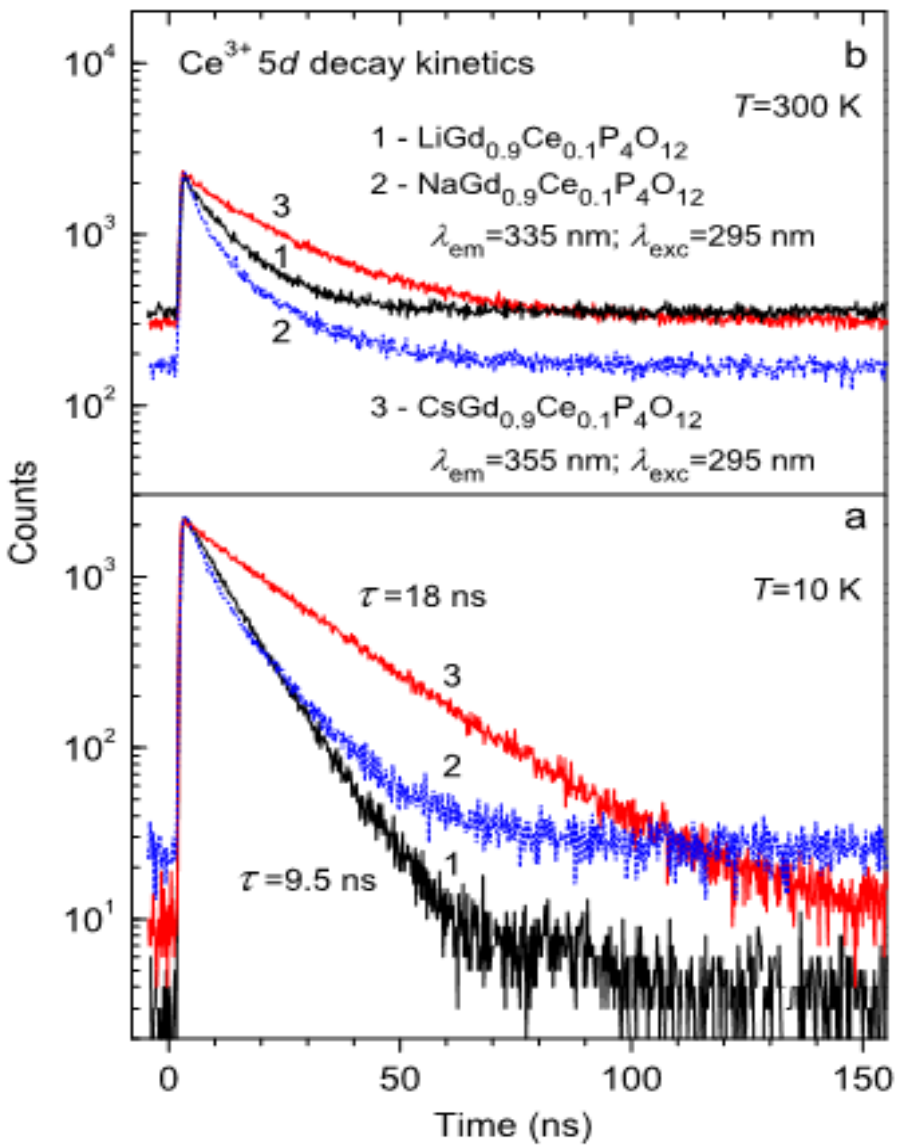

Fig. 9 Decay kinetics of the $Ce3^+$ 5d-4f luminescence from $LiGd_{0.9}Ce_{0.1}P_4O_{12}$ (curves 1), $NaGd_{0.9}Ce_{0.1}P_4O_{12}$ (curves 2) and $CsGd_{0.9}Ce_{0.1}P_4O_{12}$ (curves 3) measured at T=10 K (frame a) and T=300 K (frame b).

Contents lists available at ScienceDirect

Journal of Non-Crystalline Solids

journal homepage: www.elsevier.com/ locate/ jnoncrysol

Effect of alkali metal oxides on the properties of radio-photoluminescence glasses

Sijun Fan [a,b,*], Chunlei Yu [a], Dongbing He [a,b], Kefeng Li [a,b], Lili Hu [a]

Sample no.	$LiPO_3$	$NaPO_3$	KPO_3	$Al(PO_3)_3$	Ag_2O	$\rho\pm$ 0.0002	$Z_{eff}\pm$ 0.01	$n_d\pm$ 0.00002
1	70	-	-	30	0.5	2.5374	12.10	1.52628
2	-	70	-	30	0.5	2.60	12.27	1.50923
3	-	-	70	30	0.5	2.5065	13.91	1.49669

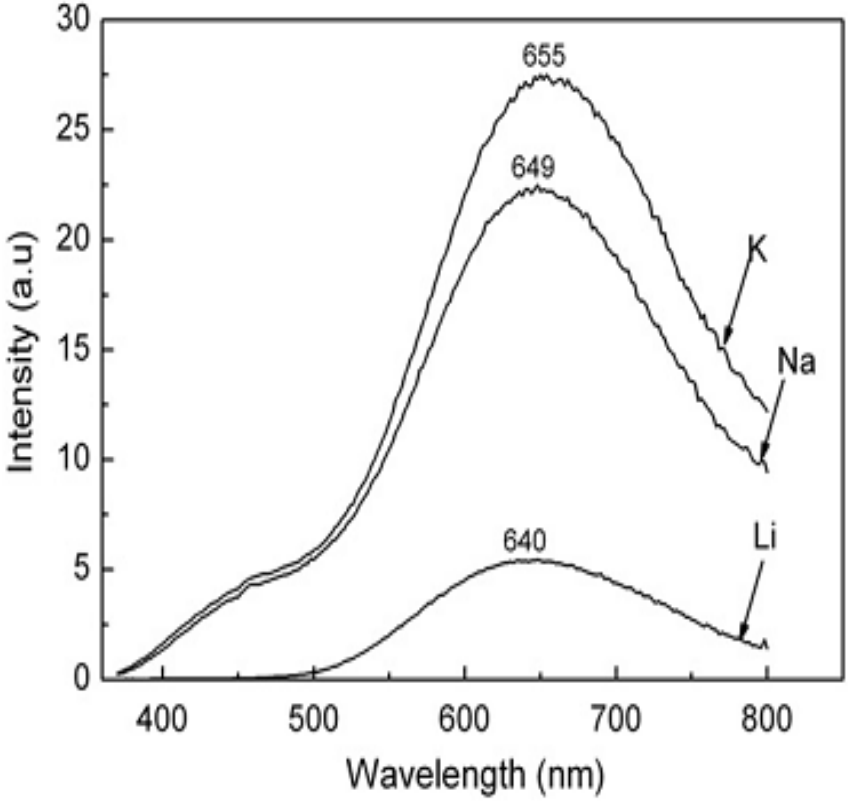

The ligand field strength of Mn^{2+} increases and the emission bands are red-shift with increasing the radius of other modifiers in glass network. In a similar manner, the ligand field of Ag may be influenced by that of other modifiers (e.g., Li, Na, and K) in this experiment. It becomes strong due to the decrease of the radius of alkali ions in glass network. Thismeans that the emission bands of luminescence centers related to Ag may be red-shift when small alkali ions are replaced by large ones in glass network.

Fig. 10 Fluorescence spectra of alkali aluminophosphate glasses with the same silver concentration after γ irradiation.

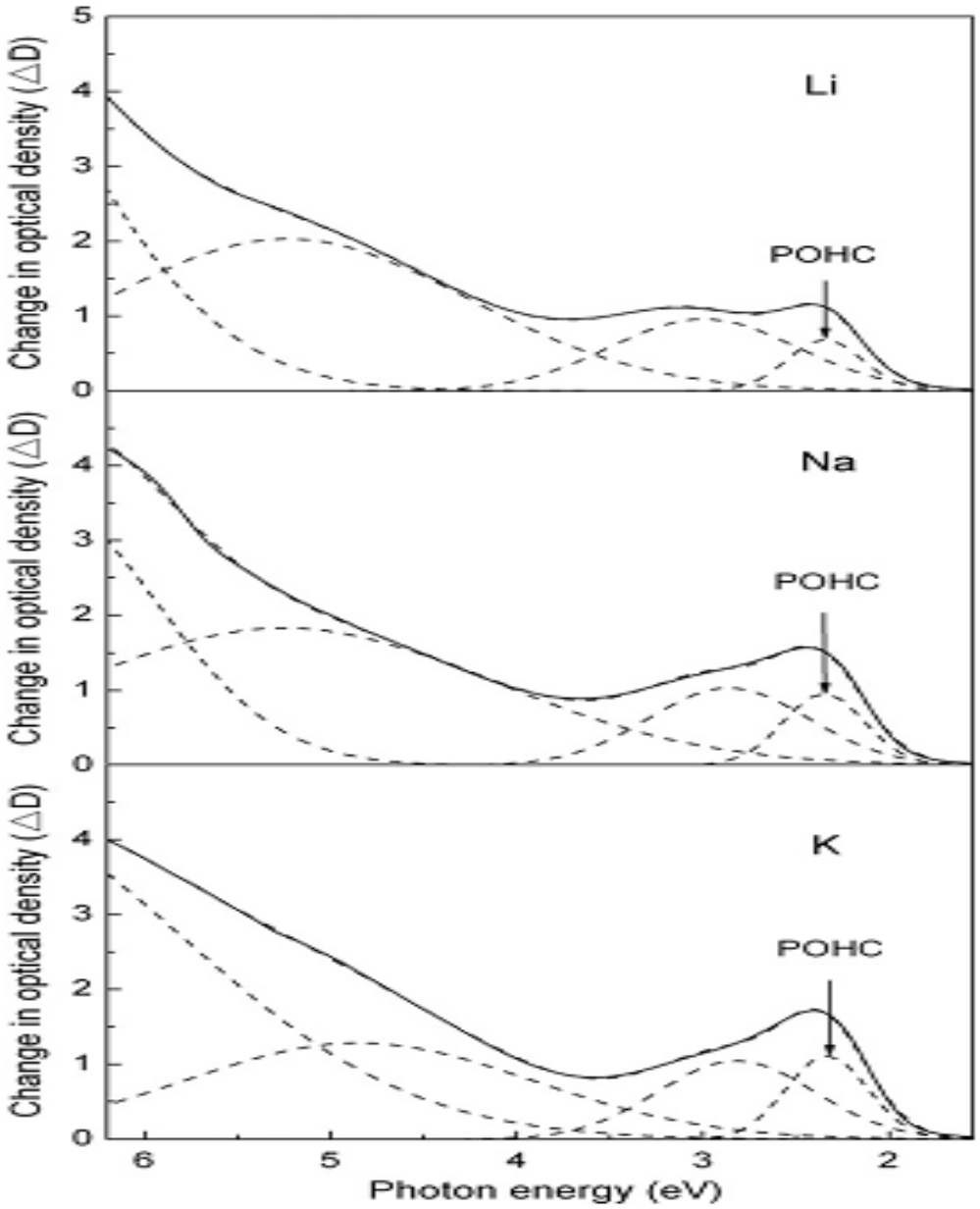

The relative RPL intensity increases in the order Li<Na<K. It is well known that the relative fluorescence intensity is proportional to the number of RPL centers which is related to the number of color centers generated in gamma-irradiated glass host. Therefore, color centers in gamma-irradiated basic glass should be investigated in detail. The resolution of induced spectra in different alkali aluminophosphate glasses are shown in Fig. 11.

Fig. 11 Gaussian resolution of induced absorption spectra in undoped glass samples with different glass modifiers.

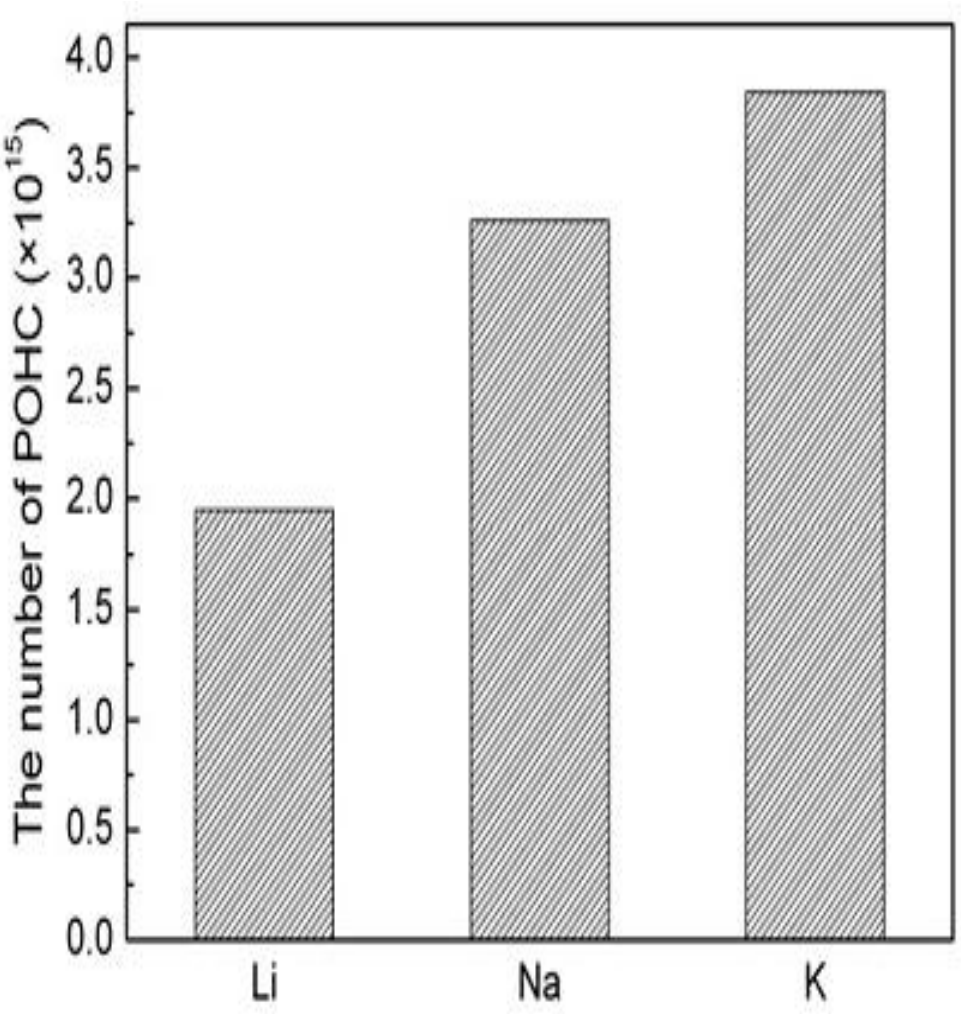

Fig. 12 Irradiation induced phosphorus oxygen hole centers (POHC) in samples with different glass modifiers. The number of POHC was calculated by formula 2 (Smakula's formula).

Fig. 12 shows that the number of POHC in gamma-irradiated basic glasses increases in the order Li, Na and K under conditions of the same irradiation dosage. The reasons are as follows: at first, the ionic field strength which affects the density of glass structure decreases in the order Li, Na and K. Secondly, the ionic of K ions is so large that they can depolymerize glass network. Thirdly, the formation of color centers is related to the coherence of glass structure and the field strength of alkali ions. The lower coherence of glass structure and field strength of alkali ions are favorable for forming color center II (POHC). As discussed above, more color centers results in more RPL centers. This is the reason that the relative RPL intensity increases in the order Li > Na > K.

Contents lists available at ScienceDirect

Physica B

journal homepage: www.elsevier.com/locate/physb

Spectroscopic and optical properties of Nd^{3+} doped fluorine containing alkali and alkaline earth zinc-aluminophosphate optical glasses

Glass	$(NaPO_3)_6$	$Zn_3(PO_4)_2$	BaF_2	AlF_3	LiF	NaF	KF	NdF_3
A	50	10	10	9	20	-	-	1
B	50	10	10	9	-	20	-	1
C	50	10	10	9	-	-	20	1

Physical property	Glass A	Glass B	Glass C
Refractive index (n_d) at 589.3 nm	1.526	1.523	1.520
Density, d (g/cm^3)	2.562	2.576	2.432
Average molecular weight $\overline{M}$ (g)	376.76	379.97	372.74
Nd^{3+} ion concentration N ($\times 10^{22}$ ions/cm^3)	0.409	0.408	0.392
Mean atomic volume (g/cm^3/atom)	8.451	8.477	8.808
Optical dielectric const ($p\partial t/\partial p$)	1.328	1.319	1.310
Dielectric const (ε)	2.328	2.319	2.310
Reflection losses (R) (%)	4.336	4.297	4.257
Molar refraction R_m (cm^{-3})	45.138	45.05	60.43
Polaron radius r_p (Å)	2.51	2.52	2.55
Interionic distance r_i (Å)	6.253	6.258	6.342
Molecular electronic polarizability α ($\times 10^{-23}$ cm^3)	1.787	1.785	2.395
Field strength F ($\times 10^{15}$ cm^{-2})	4.72	4.71	3.86
Optical basicity (Λ_{th})	0.597	0.598	0.601

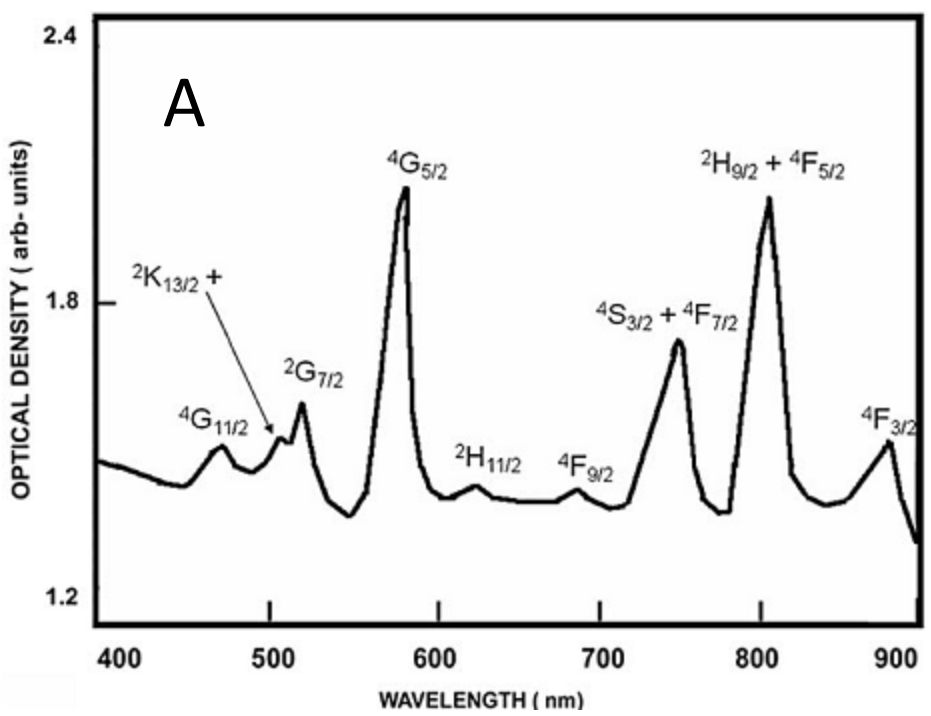

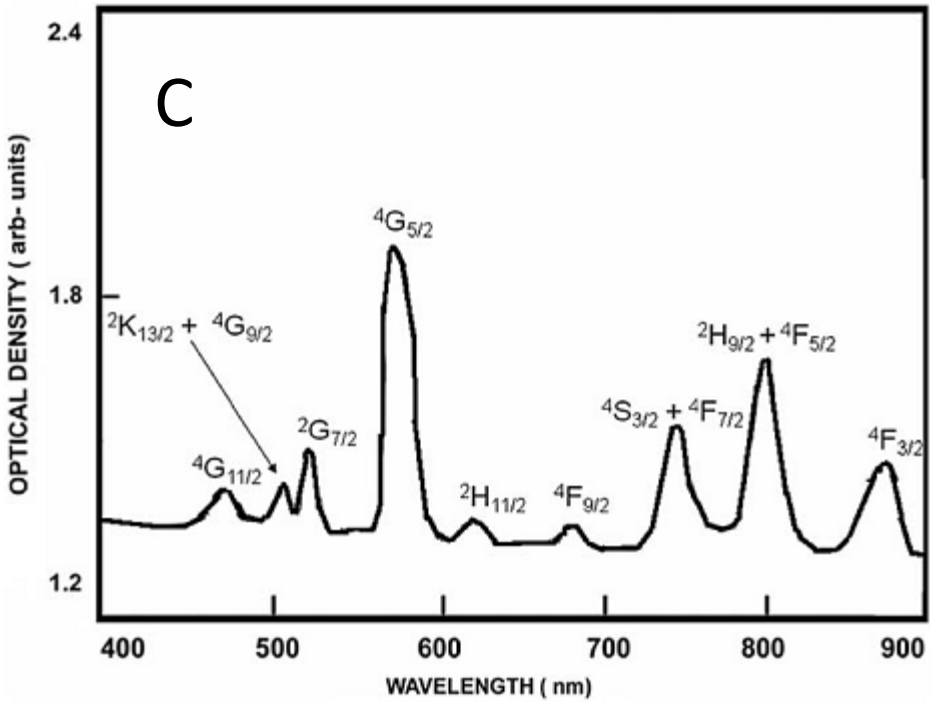

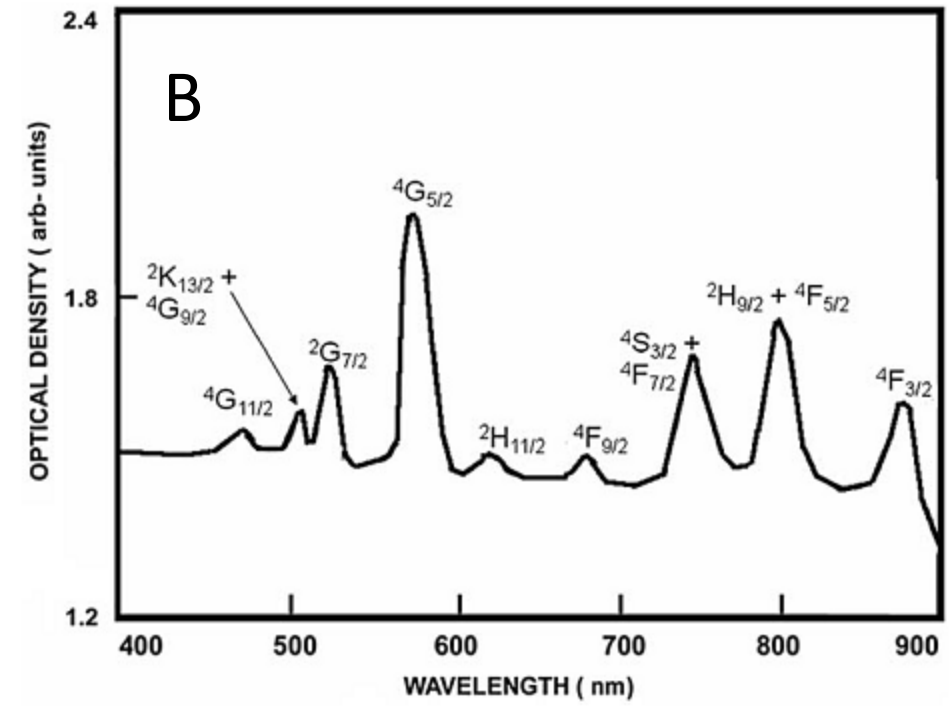

Fig. 13 Optical absorption spectrum of Glass A.

Fig. 14 Optical absorption spectrum of Glass B.

Fig. 15 Optical absorption spectrum of Glass C.

Contents lists available at SciVerse ScienceDirect

Journal of Molecular Structure

journal homepage: www.elsevier.com/locate/molstruc

Spectroscopic studies of lithium phosphate, lead phosphate and zinc phosphate glasses containing TiO_2: Effect of gamma irradiation

N.A. Ghoneim [a], A.M. Abdelghany [b,*], S.M. Abo-Naf [a], F.A. Moustafa [a], Kh.M. ElBadry [a]

Sample	P_2O_5	Li_2O	PbO	ZnO	Added (wt%)	
	mol%				TiO_2	Al_2O_3
LiPTi1	50	50			0.25	0.5
LiPTi2	50	50			0.50	0.5
LiPTi3	50	50			0.75	0.5
LiPTi4	50	50			2.50	0.5
PbPTi1	50		50		0.25	0.5
PbPTi2	50		50		0.50	0.5
PbPTi3	50		50		0.75	0.5
PbPTi4	50		50		2.50	0.5
ZnPTi1	50			50	0.25	0.5
ZnPTi2	50			50	0.50	0.5
ZnPTi3	50			50	0.75	0.5
ZnPTi4	50			50	2.50	0.5

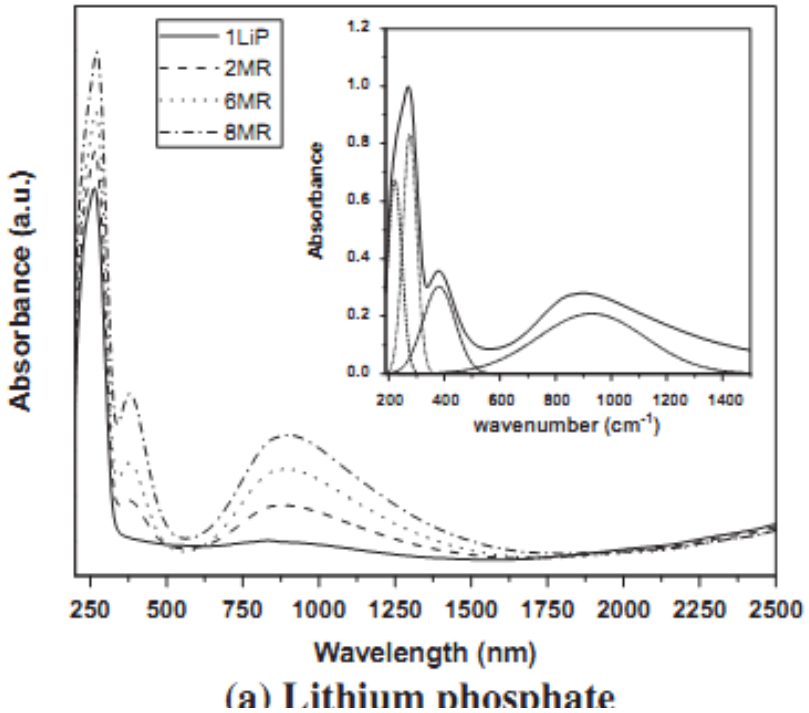

(a) Lithium phosphate

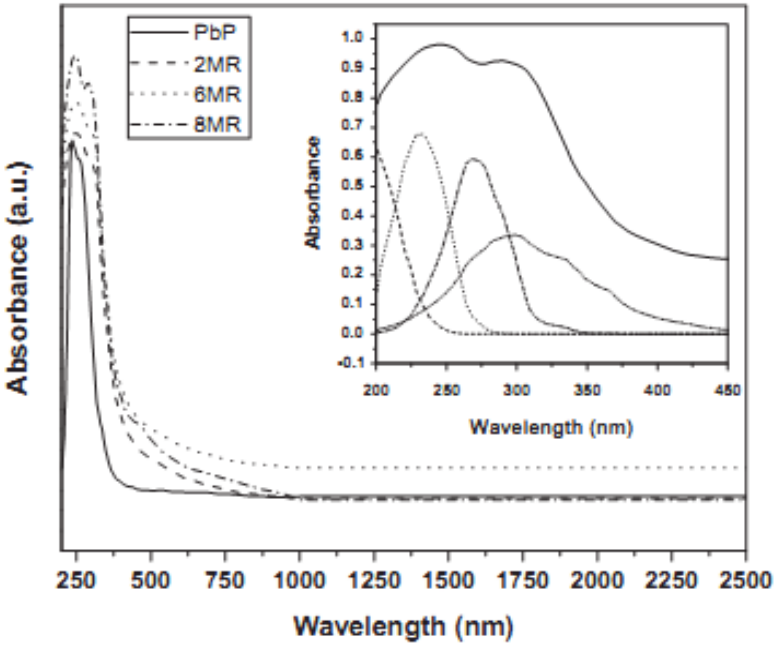

(b) Lead Phosphate

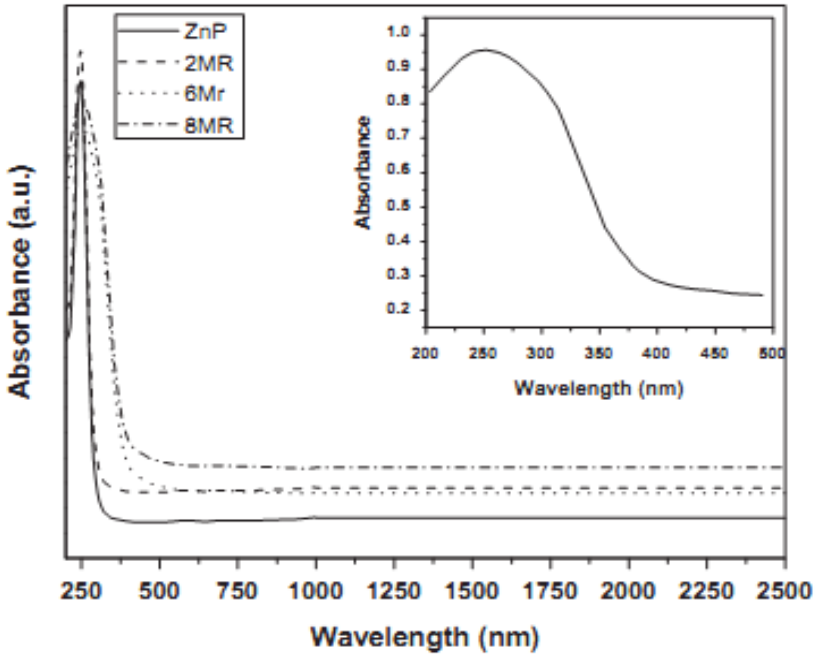

(c) Zinc phosphate

Fig. 16 Optical absorption spectra of the three base phosphate glasses.

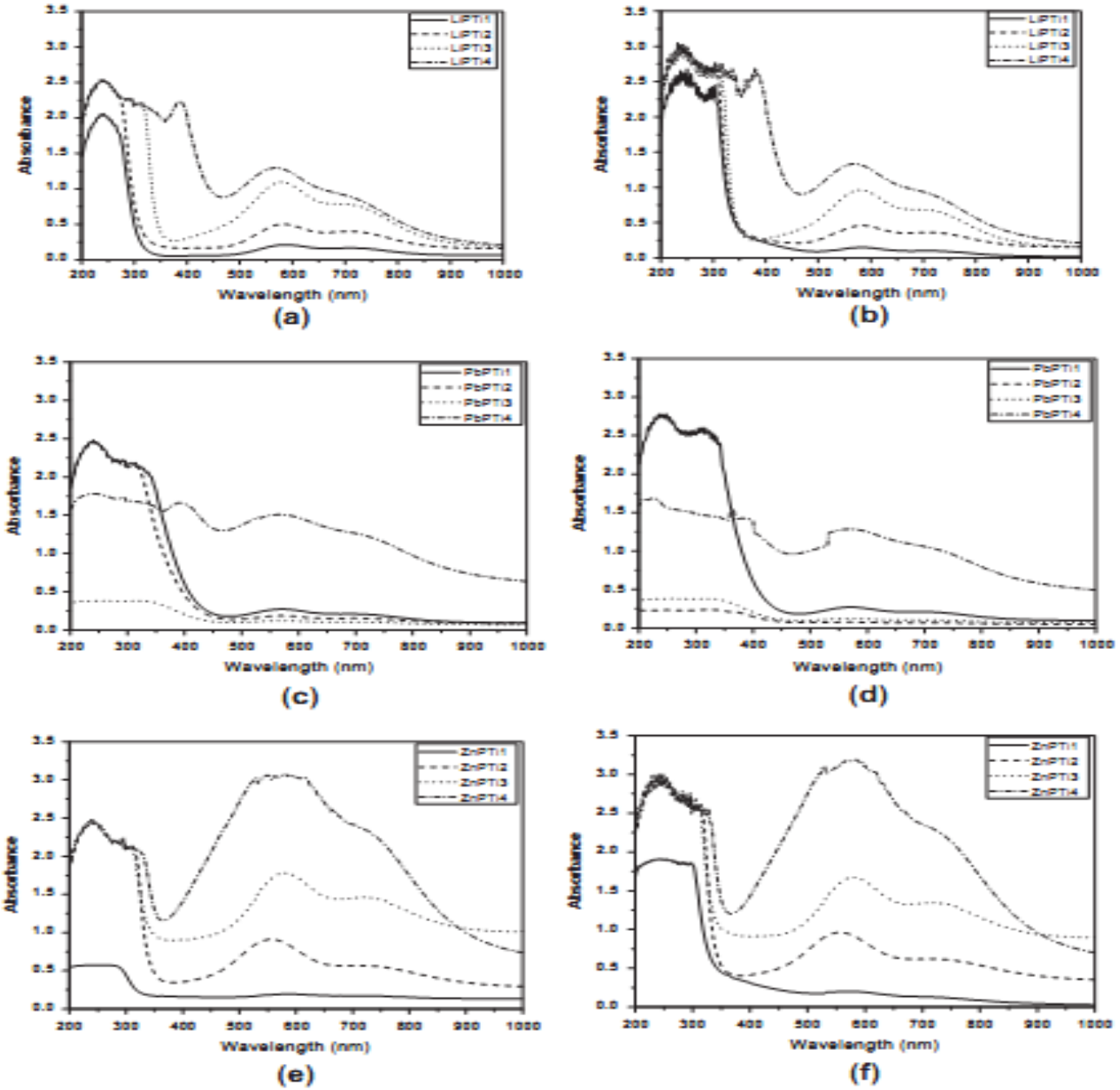

Fig. 17 Optical absorption spectra of the TiO_2-doped three phosphate glasses before and after gamma irradiation.

Next week

Course Outine:

Week 12: Glass composition, structures and applications (4)

- Other Glass
- *Case studies from international publications*